A Realistic Radar Simulation Framework for CARLA Supplementary Materials

Satyam Srivastava
BITS Pilani
f20190188@pilani.bits-pilani.ac.in

Jerry Li
UCR
jli793@ucr.edu

Pushkal Mishra
UCSD
pumishra@ucsd.edu

Kshitiz Bansal
Blue River Tech
ksbansal@ucsd.edu

Dinesh Bharadia
UCSD
dbharadia@ucsd.edu

1. Overview

The results from the main manuscript quote driving scores, route completion scores and infraction penalties among other scores, however they serve as an abstract representation of the actual performance of the end-to-end driving models, especially in high-risk situations. In this supplementary material, we provide a detailed route-wise analysis of all our models, highlight instances where the model undergoes infractions and provide driving videos for the same. We also provide videos of specific situations[1] wherein the ego vehicle is placed in a safety critical scenario and successfully avoids crashes due to enhanced spatial awareness from integrating Shenron radar [1].

Figure 1. Aerial view of Route 3, located in Carla Town 2. Image taken from here.

We have also attached a complete driving video of Route 3 with FBLR radar view, and the overview of the route can be seen in Figure 1. Additionally, we utilize the shenron to conduct an ablation study that demonstrates the significance of angular resolutions by varying the number of antennas and analyze its impact on driving performance.

[1]Due to size constraints, only the clips showing safety-critical instances from the full recordings have been included.

2. Detailed Route-wise Analysis

In the paper, we have performed evaluations on three radar views, namely Front Only, Front+Back(abbreviated as FB) and Front+Back+Left+Right (abbreviated as FBLR). We analyze how each of the model deals with four key safety traffic scenarios that occur in routes picked from the NEAT [2] paper. Additionally, we include specific cropped scenarios from the driving video to further clarify our claims. More information on the safety critical scenarios can be found here: https://leaderboard.carla.org/scenarios/.

2.1. Unprotected left turn at an intersection

This infraction type is demonstrated in Route 0, where the ego vehicle fails to detect vehicles coming straight while trying to take a left turn. This commonly occurs in the Front-Only radar model, while the FB and FBLR models don't exhibit this issue. This issue is demonstrated in Figure 2.

2.2. Crossing negotiation at a roundabout

This type of infraction is observed on Route 5 at a roundabout, where the ego vehicle fails to yield when entering the roundabout while another vehicle is approaching from the left. In some instances, a collision is narrowly avoided because the other vehicle stops, but in other cases, a crash occurs. With the Front-Only and FB radar models, collisions are observed, whereas the FBLR radar model enables the ego vehicle to accelerate and narrowly avoid a crash. This highlights the limitations of relying solely on front-facing radar data, as the ego vehicle is unable to detect vehicles approaching from the left. While the FBLR model mitigates this issue by allowing the vehicle to speed up, it

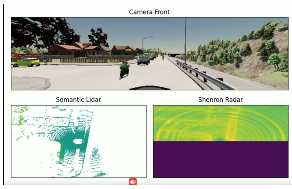

(a) Front model before the scenario

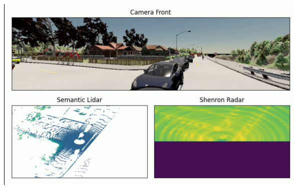

(b) Front model after the scenario

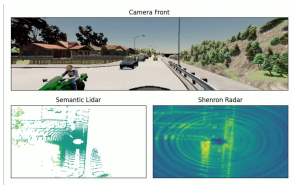

(c) FBLR model before the scenario

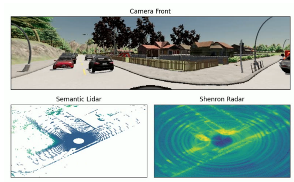

(d) FBLR model after the scenario

Figure 2. Comparison of driving video for Front and FBLR: (a) Before the safety scenario in Front model, (b) After the safety scenario in Front model, (c) Before the safety scenario in FBLR model, (d) After the safety scenario in FBLR model.

still results in a near-miss. The scenario is demonstrated in Figure 3.

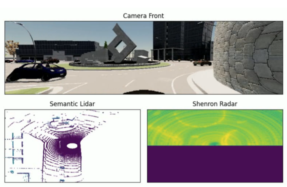

(a) Front model before the scenario

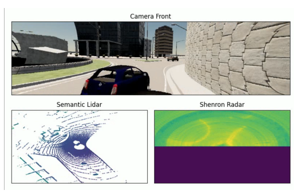

(b) Front model after the scenario

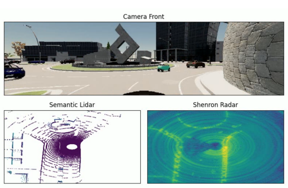

(c) FBLR model before the scenario

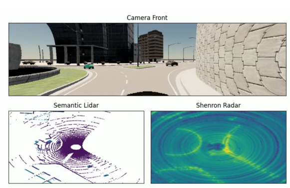

(d) FBLR model after the scenario

Figure 3. Comparison of driving video for Front and FBLR: (a) Before the safety scenario in Front model, (b) After the safety scenario in Front model, (c) Before the safety scenario in FBLR model, (d) After the safety scenario in FBLR model.

2.3. Right turn at intersection with crossing traffic

This type of infraction is observed on Route 10, where the ego vehicle fails to yield to incoming traffic from the left while attempting a right turn at an intersection. This behavior is seen in the Front-Only and FB radar models but not in the FBLR model. Depending on the timing of the traffic, the ego vehicle may avoid a collision if it begins the turn during a gap in traffic directly ahead. However, it remains at risk of a crash due to vehicles approaching from the left. Incorporating the left radar view in the FBLR model mitigates this issue by providing a wider field of view, allowing the ego vehicle to assess incoming traffic more effectively and proceed safely. This issue is demonstrated in Figure 4.

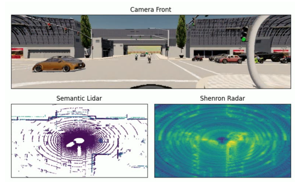

(a) FB model before the scenario

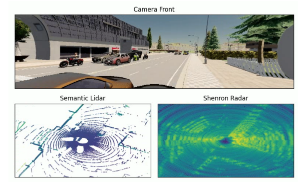

(b) FB model after the scenario

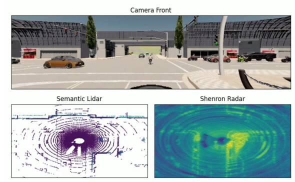

(c) FBLR model before the scenario

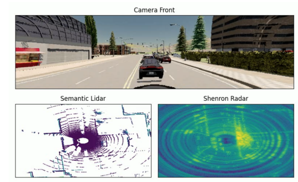

(d) FBLR model after the scenario

Figure 4. Comparison of driving video for FB and FBLR: (a) Before the safety scenario in FB model, (b) After the safety scenario in FB model, (c) Before the safety scenario in FBLR model, (d) After the safety scenario in FBLR model.

2.4. Vehicle invading lane on bend

This infraction type is demonstrated in Routes 1 and 3, where the ego vehicle struggles when navigating curved roads near iron railings. This infraction is exhibited in Front-Only radar model for both routes and only in route 3 for FB. This issue in route 3 is demonstrated in Figure 5.

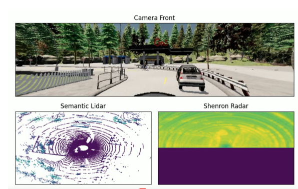

(a) Front model before the scenario

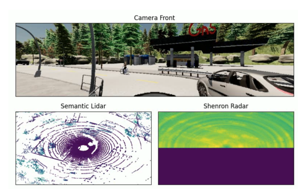

(b) Front model after the scenario

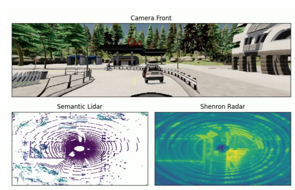

(c) FBLR model before the scenario

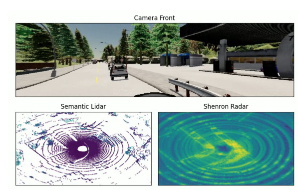

(d) FBLR model after the scenario

Figure 5. Comparison of driving video for Front and FBLR: (a) Before the safety scenario in Front model, (b) After the safety scenario in Front model, (c) Before the safety scenario in FBLR model, (d) After the safety scenario in FBLR model.

3. Resolution in Radar Sensor

The resolution of a radar sensor determines its capability to differentiate between nearby targets, which is an essential aspect affecting the radars performance in scenarios like autonomous driving, defense, and imaging systems. Radar resolution is generally divided into Range, Doppler, and Angular resolution, with angular resolution being especially crucial for modern imaging radars. In our ablations, we modify the angular resolution of the radar sensor in the Shenron simulator and perform evaluations after re-training the model with this low resolution radar. We have also attached a full length video of Route 6 for the FBLR view.

3.1. Modifying the Angular Resolution

Angular resolution in context of radars refers to the minimum angular separation at which a radar system can distinguish between two equally sized targets located at the same distance. It mainly depends on the width of the radar beam, which in-turn depends on the antenna array configuration and the wavelength of the radar signal. A key rule of thumb for angular resolution at boresight is:

$$\Delta\theta = \frac{2}{N}$$

Here, N being the number of antennas in the array. A larger number of antennas improves angular resolution by narrowing the beam-width, allowing the radar to detect finer details in its environment. For instance, Texas Instruments (TI) radar sensor [3] incorporates 86 linear antenna arrays, achieving high angular resolution suitable for advanced imaging applications, whereas radars like Radarbook [4], with 16 antenna arrays, provide lower angular resolution, making them less effective for detailed analysis.

To highlight the importance of angular resolution, we use the Shenron simulation framework to compare the performance of high-resolution radar sensor (86 linear antenna array) and low-resolution radar sensor (16 linear antenna array). While the main paper focuses on evaluations using high-resolution radar sensor, this study presents evaluations using low-resolution radar sensor.

Figure 6 shows a comparison of the radar images obtained from the Shenron framework. Here, we generate both the low and high resolution radar view for the same scene of the vehicle, making it very clear that latter configuration has a higher angular resolution than the former radar configuration.

3.2. Driving Results

As previously mentioned, we use the low resolution radar and retrain the models for Front, Front+Back, and FBLR radar views. We further evaluate the routes from the NEAT [2] paper to maintain consistency, with the FB model with

(a) Camera View

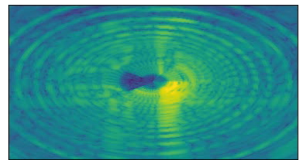

(b) Low Resolution Radar View

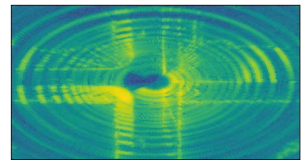

(c) High Resolution Radar View

Figure 6. Comparison of radar image for a given scenario: (a) Camera View, (b) Radar view with 16 linear antenna array, (c) Radar view with 86 linear antenna array.

86 antennas serving as the baseline for comparison, as it performed the best in terms of driving score.

Radar View	DS ↑	RC ↑	IS ↑
Front	**73.82 ± 4.94**	91.56 ± 2.26	**0.79 ± 0.04**
Front+Back	72.75 ± 6.85	**92.61 ± 0.94**	0.75 ± 0.07
FBLR	54.23 ± 5.84	80.69 ± 4.65	0.64 ± 0.06
Front+Back (86 Rx)	82.39 ± 4.87	97.03 ± 2.95	0.84 ± 0.03

Table 1. Results for different radar views using 16-antennas with Driving Score (DS), Route Completion (RC) and Infraction Score (IS).

As the results indicate from Table 1, the high-resolution FB model achieves much better results when compared to low-resolution radar configurations, mainly because of having more infractions (lower infraction score). Also we observe that increasing the number of radar views paradoxically degrades performance, as evidenced by the FBLR having substantially lower driving score. This can be attributed to the blurry and imprecise nature of low-resolution radar views, which becomes problematic when multiple views are stitched together. Also a visual comparison between the two radar views from Figure 6 reveals markedly different levels of clarity and detail, explaining why simpler configurations like Front-only model outperform FBLR.

Radar View	Veh ↓	Stat ↓	Red ↓	Dev ↓	TO ↓
Front	**0.58 ± 0.21**	0.09 ± 0.04	**0.04 ± 0.06**	0.19 ± 0.08	0.14 ± 0.09
Front+Back	1.08 ± 0.26	**0.03 ± 0.04**	0.06 ± 0.05	**0.09 ± 0.08**	**0.09 ± 0.09**
FBLR	2.21 ± 1.13	1.70 ± 0.93	0.11 ± 0.04	1.7 ± 0.93	0.49 ± 0.11
Front+Back (86 Rx)	0.43 ± 0.12	0.01 ± 0.02	0.05 ± 0.04	0.01 ± 0.03	0.00

Table 2. Results for different radar views using 16-antennas with Vehicle Infractions (Veh), Static Object Collisions (Stat), Red Light Infractions (Red), Route Deviations (Dev) and Agent Time Outs (TO).

Scores from Table 2 again reinstate the point that the high resolution outperforms all other models that use low resolution radar. Also the FBLR model suffers the most infractions as compared to Front and FB models, which suggest that higher radar resolution with focused directional coverage is more effective than distributed low-resolution coverage for autonomous driving applications.

4. Conclusion

The FBLR radar configuration demonstrates superior performance in most safety-critical traffic scenarios compared to Front-Only and FB configurations. This is mainly because the FBLR configuration provides a wider field of view, allowing the ego vehicle to better assess its surroundings and make safer decisions in complex traffic situations.

We also emphasize the crucial role of angular resolution in radar sensor performance. The advantages of high-resolution radar sensors, facilitated by larger antenna arrays, demonstrates how simulation frameworks can effectively evaluate and optimize radar designs for specific needs. These findings underscore the importance of carefully considering radar sensor configuration and resolution in the development of autonomous driving systems. Note that we will be releasing the radar dataset collected, code and all evaluation videos upon acceptance of this paper.

References

[1] Kshitiz Bansal, Gautham Reddy, and Dinesh Bharadia. Shenron - scalable, high fidelity and efficient radar simulation. *IEEE Robotics and Automation Letters*, 9(2):1644–1651, 2024. 1

[2] Kashyap Chitta, Aditya Prakash, and Andreas Geiger. Neat: Neural attention fields for end-to-end autonomous driving. In *Proceedings of the IEEE/CVF International Conference on Computer Vision*, pages 15793–15803, 2021. 1, 3

[3] Texas Instruments Incorporated. *Imaging Radar Using Cascaded mmWave Sensor Reference Design*. Tidep-01012 edition, 2019. 3

[4] INRAS. Radarbook2. 3